

# Effect of Alumina/Iron Catalysts with the Use of Different Ferrous Compounds on the Formation of Carbon Nanotubes

Xiaoxue Zhang<sup>\*1</sup>, Juha-Pekka Nikkanen<sup>1</sup>, Jyri Rintala<sup>2</sup>, Mika Pettersson<sup>2</sup>, Tomi Kanerva<sup>1</sup>, Jarmo Laakso<sup>1</sup>, Erkki Levänen<sup>1</sup>, Tapio Mäntylä<sup>1</sup>

<sup>1</sup>Department of Materials Science, Tampere University of Technology, P.O. Box 589, FI-33101 Tampere, Finland

<sup>2</sup>Nanoscience Center, Department of Chemistry, University of Jyväskylä, P.O. Box 35, FI-40014 Jyväskylä, Finland

received April 15, 2010; received in revised form July 07, 2010; accepted July 15, 2010

## Abstract

Two different ferrous compounds, iron nitrate and ferrocene, were applied as the iron precursor in sol-gel processing in order to produce two different iron-containing alumina catalysts. Methane gas was decomposed over the two catalysts under the same conditions to produce carbon nanotubes. Multi-walled carbon nanotubes were formed on the catalyst with iron nitrate, but not obtained on the catalyst produced with ferrocene. X-ray diffraction, transmission electron microscopy, field emission scanning electron microscopy, Raman spectroscopy and nitrogen adsorption/desorption characterization were performed to compare the catalysts and discuss the effect of the catalysts obtained with the different ferrous compounds on the formation of the multi-walled carbon nanotubes.

*Keywords:* carbon nanotubes, alumina, sol-gel method, chemical catalytic vapour deposition

## I. Introduction

Carbon nanotubes (CNTs) are a relatively young and new class of materials that have attracted tremendous attention since their discovery in 1991 thanks to their extraordinary structural, electronic, mechanical and chemical properties. They have therefore been intensively studied with regard to their synthesis, characterization and applications<sup>1-10</sup>. Many methods have been reported for synthesizing carbon nanotubes. Of these methods, chemical catalytic vapour deposition (CCVD) has the major advantages of low cost, easy scale-up, high yield of carbon nanotubes and moderate temperature of less than 1000 °C<sup>2-6</sup>. In CCVD, various hydrocarbons such as CH<sub>4</sub>, C<sub>2</sub>H<sub>6</sub>, C<sub>2</sub>H<sub>4</sub> and C<sub>2</sub>H<sub>2</sub> have been used as a carbon source over catalysts of Fe, Ni, Co or Fe-Ni supported on alumina, silica and other materials<sup>4, 7-9</sup>. The formation of carbon nanotubes in good quality and quantity depends to a large extent on the catalytic properties of the catalysts, i.e. the interaction between the support and the metal particles, which in turn is dependent on the preparation methods, pre- and post-synthetic treatments and the presence of other active components and their percentage, etc.<sup>8, 10</sup>.

The sol-gel method is a good way to synthesize catalysts since it allows the design of the materials (particle size, morphology, surface area, pore diameter, etc.) based on control of the process conditions (temperature, precursors, concentration of reagents, amount of water, drying, etc.)<sup>11</sup>. The sol-gel method has the advantages of high chemical purity, high chemical homogeneity, low cal-

inating temperatures and good control of particle size<sup>12</sup>. Metal-containing catalysts can be prepared by the sol-gel method by dispersing the metal precursors into solution during the support material synthesis<sup>4</sup>. Sol-gel synthesis may introduce unique metal-oxide interactions or oxide-oxide interactions, which will influence the catalytic properties of the catalysts<sup>13</sup>.

We studied the synthesis of nanocrystalline transition aluminas ( $\gamma$ -,  $\delta$ -,  $\theta$ -alumina) in the morphologies of nanoparticles and nanorods<sup>14</sup>. And we also obtained nanocrystalline  $\alpha$ -alumina with novel morphology at a relatively low temperature of 1000 °C for 40 h<sup>15-16</sup>. In this study, we prepared alumina/iron catalysts by modifying the sol-gel synthesis of alumina. Two different ferrous compounds, iron nitrate and ferrocene, were used as the iron source. Methane gas was decomposed over the two catalysts in the same conditions to produce carbon nanotubes. Multi-walled carbon nanotubes were formed on the catalyst when iron nitrate was used, but not obtained when ferrocene was used. The two catalysts obtained from different precursors were characterized and compared in order to tentatively discuss the influence of the ferrous precursors on the formation of the carbon nanotubes.

## II. Experimental Details

The sol-gel method was used to prepare two different alumina/iron catalysts based on different ferrous compounds, iron (III) nitrate nonahydrate (FeN<sub>3</sub>O<sub>9</sub>·9H<sub>2</sub>O) and ferrocene ((C<sub>5</sub>H<sub>5</sub>)<sub>2</sub>Fe). The catalysts were prepared by introducing the ferrous compound into the process of synthesizing alumina by using aluminium tri-sec-

\* Corresponding author: [xiaoxue.zhang@tut.fi](mailto:xiaoxue.zhang@tut.fi)

butoxide ( $C_{12}H_{27}AlO_3$ ), isopropyl alcohol ( $C_3H_7OH$ ) and ethyl acetoacetate ( $C_6H_{10}O_3$ ) in accordance with a previous study<sup>15</sup>. The molar ratio of the ferrous compound to aluminium tri-sec-butoxide was 9.1 %. The gel was dried at 120 °C to obtain fine powder, which was then reacted with boiling water for 10 min and dried again into fine powder at 120 °C. The powder resulting from the use of iron nitrate is designated NB, and the powder with ferrocene is named FB. The NB and FB powders were then heat-treated at 600 °C in air for 30 min to form alumina. The heat-treated NB and FB powders were then placed in a tube furnace with a silica glass tube in order to grow carbon nanotubes on the powders. The furnace was evacuated by a Pfeiffer Balzers Uno 2.5 single-stage rotary vane vacuum pump and heated to 800 °C. Then methane gas ( $CH_4$ ) was slowly fed into the furnace until atmospheric pressure was reached. After that the flow of methane gas was stopped. The growth time of carbon nanotubes was 1 hour and no more methane was fed into the furnace during their growth. The methane-treated samples are designated NCM when the catalyst was produced with iron nitrate and FCM for the catalyst produced from ferrocene. For comparison with the methane-treated NCM and FCM powders, blank tests were conducted with the NB and FB powders heat-treated in the same conditions but without any feed of methane gas. The blank test powders are designated NC and FC based on the NB and FB powders, respectively.

The crystalline phase composition was determined by X-ray diffraction (XRD, Kristalloflex D-500, Siemens) with Cu  $K\alpha$  radiation. The morphology was examined by means of transmission electron microscopy (TEM, Jeol JEM 2010) and field emission scanning electron microscopy (FESEM, Zeiss ULTRAplus). The structures of the carbonaceous materials were studied with Raman spectroscopy using two different excitation wavelengths: 532 nm (Alphas Monolas-532-100-SM) and 632.8 nm (Melles Griot 25-LHP-991-230). The specific surface areas were calculated from  $N_2$  adsorption/desorption isotherms (Coulter Omnisorp 100 CX, Beckman Coulter Inc.) with Coulter SA-reports™ software based on the Brunauer-Emmett-Teller (BET) equation using the data in a  $P/P_0$  range of 0.05-0.4.

### III. Results and Discussion

We studied the formation of  $\gamma$ -alumina nanorods by heat-treating boehmite powder at 600 °C in a previous paper<sup>14</sup>. In this study, iron nitrate and ferrocene were introduced as the iron source to prepare the alumina/iron catalysts. The XRD patterns of the NB, FB, NC and FC powders are shown in fig. 1. NB and FB powders are those obtained after the boiling water treatment and NC and FC powders are those obtained after heat-treatment at 600 °C. The XRD pattern of FB is due to boehmite ( $\gamma$ - $AlOOH$ , JCPDS card No. 74-1895), while the XRD pattern of NB could be from boehmite, but the very broad diffraction peaks could also suggest an amorphous state in NB. After the blank tests,  $\gamma$ -alumina (JCPDS card No. 10-425) was formed in both NC and FC. In all the XRD patterns, iron-containing compounds are not observed, probably owing to the

fact that their amount is too small to be detected or they are in an amorphous state.

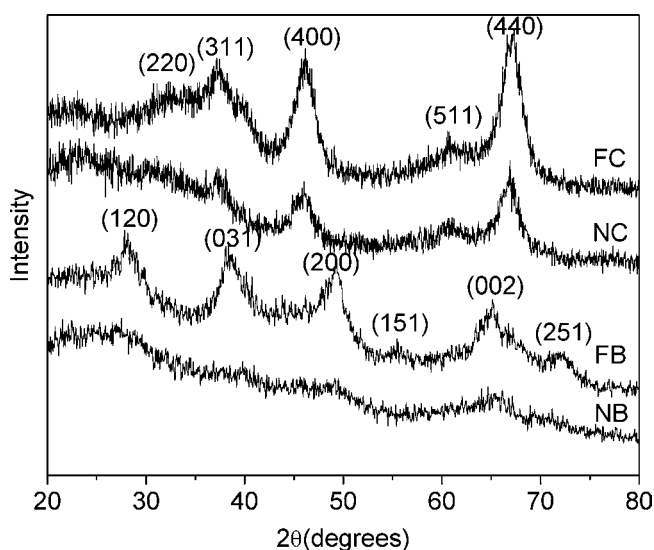


Fig. 1: XRD patterns of the NB, FB, NC and FC powders.

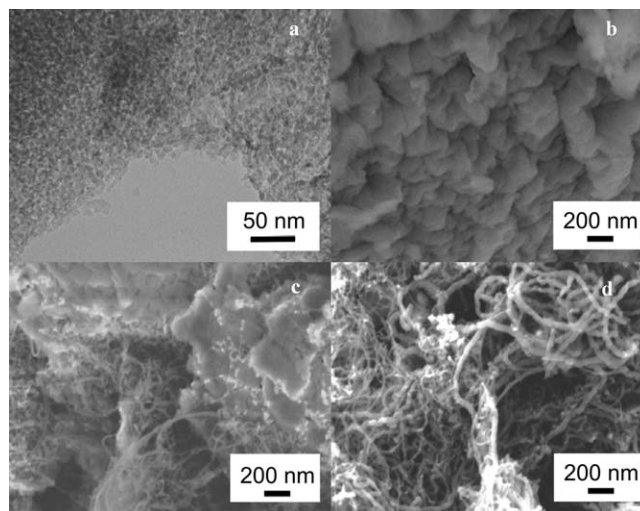


Fig. 2: Special morphology of the NC powder: (a) a TEM image and (b) a FESEM image. Bundles of carbon nanotubes from the NCM powder: (c, d) FESEM images.

NCM was prepared by treating the heat-treated NB powder with methane gas and NC was obtained in the same conditions but without feeding methane into the furnace. The only difference between NC and NCM is the use of methane gas. The morphology of the NC powder is shown in the TEM and FESEM images in figs. 2(a) and (b). The spherical particles with diameters of about 10 nm in fig. 2(a) could be crystallites of  $\gamma$ -alumina co-existing with a small amount of iron oxide. The crystallites aggregated into large crystals and the surface image of a large crystal are shown in fig. 2(b). After methane gas was fed into the furnace, bundles of carbon nanotubes could be observed as shown in figs. 2(c) and (d). Meanwhile, in fig. 2(c), shining particles of about 10-20 nm in size and carbon nanotubes can be seen on the surface of a large crystal of  $\gamma$ -alumina, which has a similar morphology to the NC powder in fig. 2(b). The shining particles with a size of about 10-20 nm are probably the reduced iron. Methane gas is decomposed at 800 °C and the iron oxide

on the surface of  $\gamma$ -alumina crystals is reduced into iron. The carbon is then dissolved into the particles of iron, oversaturated by diffusion and precipitated on the rear surface of the iron to form carbon nanotubes.

On the other hand, carbon nanotubes were not formed on FC after methane gas was fed into the furnace. No shining particles with a size of about 10-20 nm can be seen in fig. 3(a) and the morphology of the  $\gamma$ -alumina is very similar to the flaky boehmite powder described previously without using ferrous precursor in the preparation. FC was obtained by using the same conditions without methane gas, as compared to FCM. FC has the morphology of nanorods with lengths of about 50 nm and widths of about 5 nm, as shown in fig. 3(b). The surface image of a large crystal in FC is shown in fig. 3(c), which is similar to in fig. 3(a). As known, the presence of reduced iron particles is crucial for the formation of carbon nanotubes. Most probably, iron particles were not formed after the decomposition of methane, which might be due to the non-existence of iron oxide on the surface of the alumina crystals or because the heat treatment at 600 °C is not high enough to form iron oxide when ferrocene is used. Clearly the different ferrous compounds have an influence on the formation of CNTs, i.e. CNTs were formed on the heat-treated NB powder with iron nitrate but not formed on the heat-treated powder FB with ferrocene. The effect of different ferrous compounds needs to be carefully considered together with the crystalline phase of the supporting material, the amount of ferrous compound, particle size, morphology, processing method, etc.

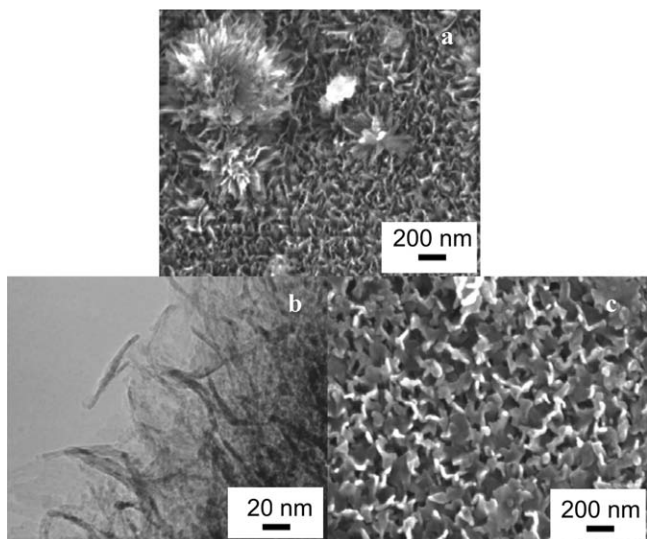


Fig. 3: Special morphology of the FCM powder: (a) a FESEM image. Morphology of FC powder: (b) a TEM image and (c) a FESEM image.

The structures of the carbonaceous materials were also studied with the help of Raman spectra. When the iron nitrate was used as iron source, the appearance of the spectrum in fig. 4(a) is characteristic for carbonaceous material, as evidenced by the G-band at 1590  $\text{cm}^{-1}$ , D-band at 1330  $\text{cm}^{-1}$  and the RBM (radial breathing mode) at 190  $\text{cm}^{-1}$ . In particular, the detection of the RBM mode, which does not appear in graphite, confirms the presence of carbon nanotubes in the sample. The RBM peak sig-

nifies the presence of CNTs with small diameters. By using the relationship of  $\omega_{\text{RBM}} = 218/d + 16$  ( $\omega_{\text{RBM}}$ : radial breathing mode frequency, d: diameter)<sup>18</sup>, the diameter is estimated to be 1.25 nm, which could correspond to the inner tube of a double-walled or a multi-walled carbon nanotube. However, when ferrocene was used as the iron source, the Raman spectrum, as shown in fig. 4(b), does not have a RBM band, and the large intensity ratio of the D to G band as well as the relatively weak G' band suggest that the sample mainly contains carbonaceous material other than MWCNTs<sup>19</sup>.

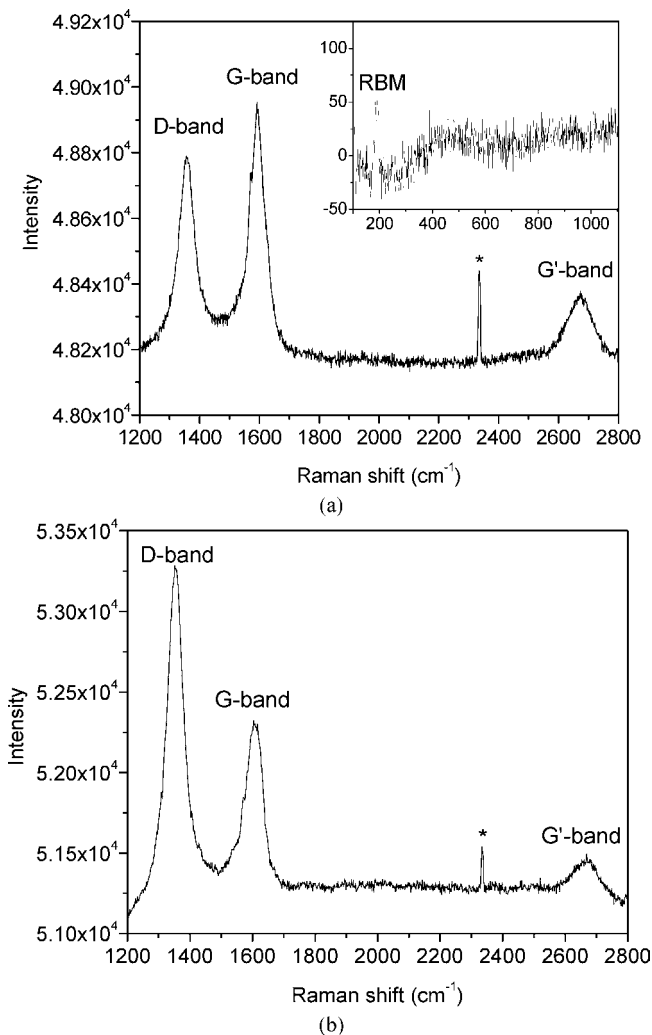


Fig. 4: Raman spectra of the NCM powder in (a) and of the FCM powder in (b) measured with 532 nm excitation. The inserted Raman spectrum in (a) was measured with 633 nm excitation. The peaks (\*) at 2330  $\text{cm}^{-1}$  are noise peaks from the testing environment, but not from the samples.

A nitrogen adsorption/desorption test was conducted to determine the isotherms and the specific surface areas of the samples, as shown in fig. 5. All the isotherms are type IV isotherms, which are related to mesopores. However, a large number of micropores exists, indicated by the adsorption at very low relative pressures in the isotherms. The isotherms in red colour are from the samples with ferrocene, and the isotherms in black colour are from the samples with iron nitrate. After reaction with water, FB and NB powders have similar shapes in their isotherms and close surface area values. After the blank tests, the surface

area of NC decreases from 261 to 119 m<sup>2</sup>/g, while that of FC decreases from 231 to 193 m<sup>2</sup>/g. After treatment with methane gas, the surface area of FCM is 248 m<sup>2</sup>/g, while the surface area of NCM is 128 m<sup>2</sup>/g. The higher surface areas of FCM and NCM than those of FC and NC are the result of the deposition of carbonaceous materials from the decomposition of methane gas. In FCM, nano-sized carbonaceous materials such as graphite and amorphous carbon were formed, resulting in a much higher surface area in the FCM than in FC. While in NCM the formation of MWCNTs did not increase the surface area much since the openings of many MWCNTs are blocked by the iron particles and the narrow inner diameters of the MWCNTs so that N<sub>2</sub> cannot adsorb into the carbon tubes, besides the carbon nanotubes measure many microns in length. Therefore the surface area of NCM is only 9 m<sup>2</sup>/g larger than that of NC since most of the carbonaceous materials are MWCNTs.

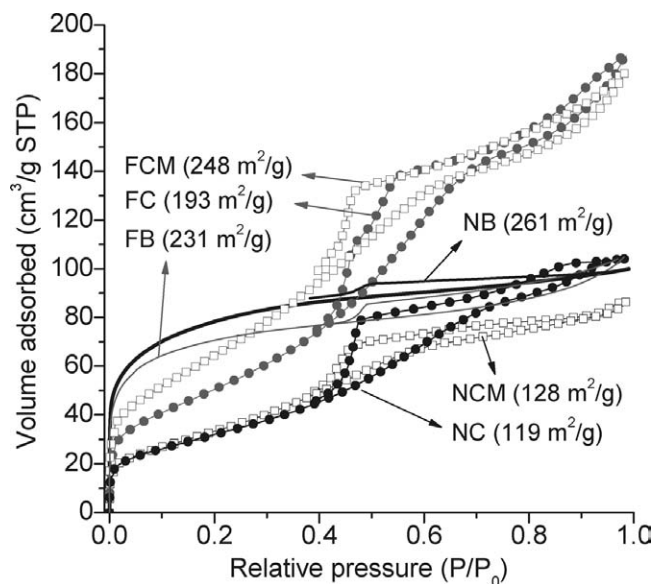


Fig. 5: Nitrogen adsorption/desorption isotherms and the corresponding surface areas of the FB, FC, FCM, NB, NC and NCM powders.

#### IV. Conclusions

Two different alumina/iron catalysts were prepared by the sol-gel method with the use of different ferrous compounds, iron nitrate and ferrocene, as the iron source. Over the heat-treated NB powder of using iron nitrate, methane gas was decomposed at 800 °C and the iron oxide on the surface of  $\gamma$ -alumina particles was reduced into iron. However, on the heat-treated FB powder with ferrocene, carbon nanotubes were not obtained, possibly owing to the non-formation of the iron particles after decomposition of the methane. The right choice of ferrous compound is therefore also an important factor for the growth of CNTs by the catalytic decomposition of methane.

#### Acknowledgments

The present study was supported by an EU research project IP NANOKER (FP6-515784-2), the Academy of Finland (decision no. 117937) and the Finnish National Graduate School on New Materials and Processes.

#### References

- Iijima, S., Helical microtubules of graphitic carbon, *Nature*, **354**, 56-58, (1991)
- Bethune, D.S., Kiang, C.H., De Vries, M.S., Gorman, G., Savoy, R., Vazquez, J., Beyers, R., Cobalt-catalysed growth of carbon nanotubes with single-atomic-layer walls, *Nature*, **363**, 605-607, (1993)
- Guo, T., Nikolaev, P., Thess, A., Colbert, D.T., Smalley, R.E., Catalytic growth of single-walled nanotubes by laser vaporization, *Chem. Phys. Lett.*, **243**, 49-54, (1995)
- Tran, K.Y., Heinrichs, B., Colomer, J.F., Pirard, J.P., Lambert, S., Carbon nanotubes synthesis by the ethylene chemical catalytic vapour deposition (CCVD) process on Fe, Co, and Fe-Co/Al<sub>2</sub>O<sub>3</sub> sol-gel catalysts, *Appl. Catal. A*, **318**, 63-69, (2007)
- Ren, Z.F., Huang, Z.P., Xu, J.W., Wang, J.H., Bush, P., Siegas, M.P., Provencio, N., Synthesis of large arrays of well-aligned carbon nanotubes on glass, *Science*, **282**, 1105-1107, (1998)
- Gan, S., Chapline, M.G., Franklin, N.R., Tomblor, T.W., Cassen, A.M., Dai, H., Self-oriented regular arrays of carbon nanotubes and their field emission properties, *Science*, **283**, 512-514, (1999)
- Fazle Kibria, A.K.M., Mo, Y.H., Nahm, K.S., Kim, M.J., Synthesis of narrow-diameter carbon nanotubes from acetylene decomposition over an iron-nickel catalysts supported on alumina, *Carbon*, **40**, 1241-1247, (2002)
- Kathyayini H., Willems I., Fonseca A., Nagy J.B. and Nagaraju N., Catalytic materials based on alumina hydroxide, for a large scale production of bundles of multiwalled (MWNT) carbon nanotubes, *Catal. Commun.*, **7**, 140-147, (2006)
- Ciambelli, P., Sannino, D., Sarno, M., Leone, C., Lafont, U., Effects of alumina phases and process parameters on the multiwalled carbon nanotubes growth, *Diamond Relat. Mater.*, **16**, 1144-1149, (2007)
- Nagaraju N., Fonseca A., Konya Z. and Nagy J.B., Alumina and Silica Supported Metal Catalysts for the Production of Carbon Nanotubes, *J. Mol. Catal. A: Chem.*, **181**, 57-62, (2002)
- Corriu R., Mehdi A. and Reye C., Nanoporous materials: a good opportunity for nanosciences, *J. Organomet. Chem.*, **689**, 4437-4450, (2004)
- Farag H.K. and Endres F., Studies on the synthesis of nano-alumina in air and water stable ionic liquids, *J. Mater. Chem.*, **18**, 442-449, (2008)
- Lecloux A.J. and Pirard J.P., High-temperature catalysts through sol-gel synthesis, *J. Non-Cryst. Solids*, **225**, 146-152, (1998)
- Zhang, X., Honkanen, M., Levänen, E., Mäntylä, T., Transition Alumina Nanoparticles and Nanorods from boehmite nanoflakes, *J. Cryst. Growth*, **310**, 3674-3679, (2008)
- Zhang, X., Ge, Y., Hannula, S., Levänen, E., Mäntylä, T., Nanocrystalline  $\alpha$ -alumina with novel morphology at 1000 °C, *J. Mater. Chem.*, **18**, 2423-2425, (2008)
- Zhang, X., Ge, Y., Hannula, S., Levänen, E., Mäntylä, T., Process study on the formation of nanocrystalline  $\alpha$ -alumina with novel morphology at 1000 °C, *J. Mater. Chem.*, **19**, 1915-1922, (2009)
- Jorio, A., Pimenta, M.A., Souza Filho, A.G., Saito, R., Dresselhaus, G., Dresselhaus, M.S., Characterizing carbon nanotube samples with resonance Raman scattering, *New J. Phys.*, **5**, 139.1-139.17, (2003)
- Araujo, P.T., Doorn, S.K., Kilina, S., Tretiak, S., Einarsson, E., Maruyama, S., Chacham, H., Pimenta, A.M., Jorio, A., Third and fourth optical transitions in semiconducting carbon nanotubes, *Phys. Rev. Lett.*, **98**, 67401, 8 pages, (2007)
- DiLeo, R.A., Landi, B.J., Raffaele, R.P., Purity assessment of multiwalled carbon nanotubes by Raman spectroscopy, *J. Appl. Phys.*, **101**, 64307-64311, (2007)